BNL-225866-2024-JAAM

GRP-ACM-82

Contribution of Speciated Monoterpenes to Secondary Aerosol in the Eastern North Atlantic

D. B. Kilgour, M. A. Zawadowicz

To be published in "ACS ES&T Air"

May 2024

Environmental and Climate Sciences Department

Brookhaven National Laboratory

U.S. Department of Energy

USDOE Office of Science (SC), Biological and Environmental Research (BER)

DISCLAIMER

Contribution of Speciated Monoterpenes to Secondary Aerosol in the Eastern North Atlantic

Delaney B. Kilgour, Christopher M. Jernigan, Shengqian Zhou, Eduardo Brito de Azevedo, Jian Wang, Maria A. Zawadowicz, and Timothy H. Bertram*

ABSTRACT: Extension of laboratory results suggests that monoterpenes, a subset of marine biogenic volatile organic compounds, might play a competitive role in secondary aerosol formation in the remote marine atmosphere, where the oxidation of dimethyl sulfide has traditionally been thought to dominate. However, the current assessment of the role of monoterpenes in secondary aerosol formation in the remote marine atmosphere is limited by the scarcity of speciated monoterpene measurements and the complete absence of collocated measurements of particle chemical composition and monoterpene speciation. Here we present measurements of gas-phase volatile organic compounds, with particular focus on speciated monoterpenes, and commensurate measurements of aerosol chemical composition in the Eastern North Atlantic. The average monoterpene concentration in periods of marine air was 14 ± 10 ppt, and the dominant isomer was β-pinene (46 ± 10%), with other contributions from α-pinene, limonene, and β-ocimene. The total monoterpene concentration in marine air was greater than that of isoprene by a factor of 3.9 on average, in contrast to prior research and potentially due to the large β-pinene contribution. Monoterpenes were significantly smaller in concentration than dimethyl sulfide, which was also highlighted by the substantial contribution of sulfate to non-refractory submicron aerosol. The mean and interquartile range of the sulfate to organic aerosol mass ratio in clean marine air were 2.7 (0.7−3.4). Finally, a simple box model analysis showed that the BVOC precursors, dimethyl sulfide, methanethiol, monoterpenes, and isoprene, could sustain the measured sulfate to organic aerosol ratio in clean marine air.

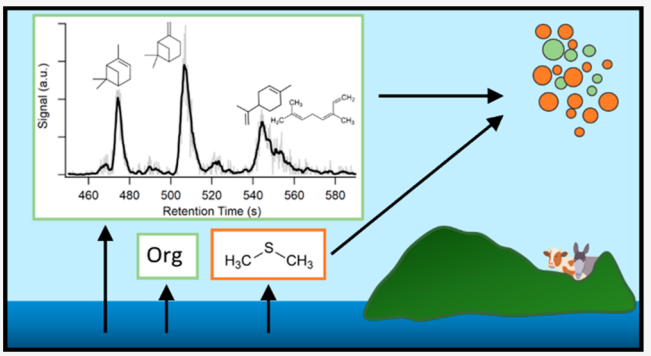

KEYWORDS: *Monoterpene, isoprene, secondary organic aerosol, sulfate, marine, ocean-atmosphere*

1. INTRODUCTION

The ocean is a source of volatile organic compounds (VOC), including organosulfur molecules like dimethyl sulfide (DMS) and methanethiol (MeSH),[1] and non-sulfur organics, including terpenes, oxygenated VOC, amines, and halocarbons.[2,3] The emission and oxidation of these reactive trace gases regulate oxidant loadings,[3,4] the production of secondary aerosol and their growth to cloud condensation nuclei sizes,[5,6] and cloud properties.[7−9] Secondary aerosol formation in marine environments is thought to be driven by the oxidation of DMS leading to the formation of the condensable products sulfuric acid and methanesulfonic acid,[7,10−12] with the oxidation of terpenes and other organics contributing less. This idea stems in part from the large and relatively well-constrained emission inventories for DMS, currently estimated at 27.1 Tg S yr^{-1}.[13]

However, findings from several recent field studies in remote marine environments challenge this assumption. For example, in the Arctic, Willis et al. (2016) measured the growth of small particles into sizes greater than 50 nm, and the event was correlated with the presence of organic species.[14] In the Eastern North Atlantic, Zheng et al. reported that 24% of 62 observed growth events over a 14-month period were driven by organics.[15] Both studies lacked collocated measurements of the chemical precursors but hypothesized the source of condensable material was marine biogenic VOC (BVOC, e.g., terpenes)[14,15] or abiotic oxygenated VOC (e.g. alkanals)[15] produced at the air-sea interface via photolysis or ozone deposition.

While heterogeneous reactions at the ocean surface can lead to the production of oxygenated VOC including alkenals and alkanals at high yield,[16−19] little is currently known about the potential of these molecules to form secondary organic aerosol (SOA) in low NO_x regimes characteristic of the marine

atmosphere. On the contrary, the oxidation of marine biogenic organics such as monoterpenes (MT) and isoprene is comparatively well-studied due to the ubiquitous source of terpenes in terrestrial environments where NO_x is similarly low and where their oxidation leads to the rapid formation of highly oxygenated molecules (HOM) and drives particle formation and growth.[20−23] MT react with the hydroxyl radical (OH) and ozone (O_3) at least an order of magnitude faster than DMS,[24] and their reactions with O_3 can form HOM at up to 5% molar yield and SOA at up to ∼20% molar yield.[21,25] Given the open questions regarding the extent to which organics contribute to secondary aerosol formation in marine environments and the large body of laboratory work constraining isomer-specific MT oxidation, we focus the following analysis on measurements of marine MT and their relative potential to contribute to secondary aerosols in the remote marine atmosphere.

A variety of MT isomers have been measured in laboratory monoculture studies of marine phytoplankton, with production rates dependent on phytoplankton speciation and external environmental stressors, including solar irradiance, temperature, and nutrient availability.[26−28] Meskhidze et al. conducted temperature- and light-dependent experiments for two diatom species and found a strong temperature dependence in α-pinene production rates that peaked before falling off at higher temperatures near 26−30 °C.[28] These studies also showed that MT production rates are often at least an order of magnitude lower than isoprene production rates for comparable experimental conditions.[27,28] Many of the same MT isomers measured in phytoplankton monoculture experiments are also emitted from terrestrial plants[29] and can have light- and temperature-dependent emission patterns.[30] One noted difference is that marine MT can be halogenated due to the high dissolved concentration of halides and are more likely to be acyclic than terrestrial MT.[31,32]

MT have been measured in the marine atmosphere during a handful of field studies.[26,33−39] Given the large terrestrial source of MT, marine MT datasets must be collected on remote cruise transects or carefully quality-controlled. Few marine MT field measurements exist to date reporting isomer-specific measurements. In the Southern Atlantic Ocean, Yassaa et al. (2008) observed α-pinene to be the overwhelmingly dominant isomer and measured its concentration at up to 225 ppt in blooming, highly biologically active waters.[26] However, all MT values were at or below their detection limits (1−5 ppt, isomer-dependent) in regions with low biological activity. They found that α-pinene was moderately correlated with chlorophyll-*a* and isoprene, which ranged from approximately five times greater than MT to roughly equivalent. Hackenberg et al. (2017) measured six MT isomers on cruises in the Atlantic and Arctic Oceans and reported significantly lower total MT concentrations of on average up to 7 ppt.[35] All MT isomers were present in similarly low concentrations in the Arctic; in the Atlantic, the dominant MT isomer was limonene, with contributions from two acyclic isomers, myrcene and ocimene. This work observed no correlation between MT and isoprene or any water-side biological indicators. Further, while not in the remote ocean, Uning et al. (2021) reported sea to air fluxes of speciated monoterpenes, averaging 51% β-pinene, 33% α-pinene, and 17% limonene based on cartridge sampling in an upwelling region off the east coast of Peninsular Malaysia; isoprene flux was approximately twice as large as the total MT flux and was well-correlated.[37] Lastly, Tokarek et al. (2017) reported measurements of speciated monoterpenes from Vancouver Island and showed that near-shore kelp vegetation can be a limonene source, though emission rates from kelp and associated diurnal-dependencies are not yet known.[38,39]

At present, there are too few measurements of MT concentrations and emission rates available to adequately constrain the spatiotemporal and biogeochemical variability in marine MT emission fluxes. As a result, parametrizations of MT emission rates are highly uncertain. A GEOS-Chem study estimated the global marine MT flux to be 0.01−29.5 Tg C yr^{-1} from bottom-up and top-down methods,[40] respectively, where the top-down estimate was based on the α-pinene measurements by Yassaa et al. (2008). However, using the dissolved, speciated MT measurements by Hackenberg et al. (2017), the oceanic MT flux term was more recently estimated at 0.16 Tg C yr^{-1}.[35] Additionally, without more speciated measurements, it is difficult to constrain how these flux estimates influence aerosol production and atmospheric reactivity.

Here we present measurements of marine BVOC concentrations, focusing on speciated monoterpenes in the Eastern North Atlantic. This dataset was collected by a Vocus proton transfer reaction mass spectrometer coupled to an online gas chromatograph during the Aerosol Growth in the Eastern North Atlantic study on Graciosa Island, Azores during Summer 2022. The measurements provide the first reported observations of MT in this region and are used to investigate biogeochemical controls on MT speciation and concentration in different marine air masses. We last evaluate the extent to which MT are a competitive secondary aerosol source in clean marine air at this site, relative to the sulfur species DMS and MeSH and other organics.

2. MATERIALS AND METHODS

2.1. Site Description. Measurements took place June 1, 2022 to July 15, 2022 (day of year (DOY) 152−196), at the Eastern North Atlantic (ENA) Atmospheric Radiation Measurement (ARM) Facility on Graciosa Island, Azores, Portugal. The site is located on the island's northern coast, approximately 400 m from the shore and roughly 100 m from the runway of Graciosa Airport. A pollution flag (Supporting Information S1) was developed for this study using continuous measurements of tracer molecules at the site. VOC observations reported represent clean air, as defined by this flag.

2.2. VOC Measurements by RT-Vocus and GC-Vocus. A Vocus proton transfer reaction time-of-flight mass spectrometer (Vocus; Aerodyne Research, Inc. and Tofwerk AG)[41] (E/N 141 Td) made continuous measurements of VOC at a 10 m sampling height through a 3/8″ O.D., 1/4″ I.D. 19 m long perfluoroalkoxy alkane (PFA) tube that was heated to 30 °C. The full inlet tube was pumped at 5.2 L/min (lpm), with the Vocus subsampling 0.1 lpm through a tee immediately in front of the Vocus capillary inlet. Isotopically-labeled dimethyl sulfide (d3-DMS) from a gas cylinder standard (1.140 ppm ± 5% d3-DMS; Airgas) was continuously added to the top of the inlet to track changes in instrument sensitivity, resulting in a constant d3-DMS concentration of 550 ppt. Instrument backgrounds were determined by overflowing the full inlet tube with zero air from a zero-air generator (Sabio 1001) for four min every 30 min.

A gas chromatography (GC) system with *in situ* thermal desorption preconcentration was coupled to the Vocus (Aerodyne Research, Inc.) for isomer-specific VOC detection of C_5-C_{12} VOC and C_2-C_{10} OVOC.[42] 1.5 or 3 L of sample air was subsampled at 0.15 lpm from the main inlet through a tee directly in front of the GC inlet. Sample passed through a heated sodium sulfite (Na_2SO_3) oxidant trap designed to remove O_3, then into a multibed sorbent tube (Tenax TA/Graphitized Carbon/Carboxen 1000, Markes International), and finally into a multibed cold trap (Tenax TA/Carbopack X/Carboxen 1003, Markes International). The flow was injected onto a GC column (MXT-624, Restek), which followed a programmed temperature ramp from 35−225 °C.

Data collection was split between sampling ambient air in real-time directly through the Vocus (RT-Vocus), saved at 1 Hz, and sampling ambient air first through the coupled GC preconcentration system (GC-Vocus), with chromatographic separation saved at 5 Hz. Each day consisted of primarily RT-Vocus collection, with two to four ambient and zero air chromatograms collected by the GC-Vocus to capture isomer-specific diurnal profiles. Extra details on ambient measurements are in Supporting Information S2.

RT-Vocus was used to quantify DMS, MeSH, and total MT, while GC-Vocus was used to quantify isoprene and speciate the quantified MT. The GC-Vocus was required for quantifying isoprene due to non-isoprene molecules fragmenting to the RT-Vocus molecular ion for isoprene. RT-Vocus limits of detection for DMS, MeSH, and MT at a signal-to-noise ratio of 3 at 5 min averaging time were 1.8, 5.1, and 2.5 ppt, respectively.[43] GC-Vocus isoprene limit of detection was 6.8 ppt for 1.5 L preconcentration and 2.0 ppt for 3 L preconcentration.[42]

The major MT isomers (α-pinene, β-pinene, and limonene) (accounting for on average 96% of the total GC-Vocus MT signal) were identified via monoterpene standards. We note that there exist numerous MT isomers in the NIST Chemistry WebBook expected to elute in a narrow retention time range, and all identifications are best assignments based on standards, retention indices, and speciation reported in the literature. Limonene is reported as a combined peak with β-ocimene, as they eluted too close to each other for separable peak fitting (Fig. S2). MT isomers were assumed to have equivalent sensitivity, meaning the fractional MT isomer contribution was based on the peak area. More details on calibration factors, VOC uncertainties, the decision to quantify isoprene with the GC-Vocus,[44] and isomer identification are in Supporting Information S3−S4 and Fig. S1−S3.

2.3. Supporting Measurements. Several continuous measurements at ENA provided by ARM[45] were utilized in this analysis, including aerosol chemical composition,[46] carbon monoxide (CO),[47] O_3,[48] and meteorological properties,[49] all measured from a 10 m inlet height. Chemical composition of non-refractory aerosol was measured with an aerosol chemical speciation monitor (ACSM; Aerodyne Research, Inc.) and was corrected for composition-dependent collection efficiency.[50] ACSM detections limits were assumed to be equivalent to those reported in the literature, resulting in 30 min detection limits of 0.148 μg m^{-3} for organic aerosol and 0.024 μg m^{-3} for sulfate aerosol.[51] Points below the detection limit were replaced with half the detection limit for interpretation of the sulfate/organic ratio and for reporting statistics.[52] A sensitivity test evaluating how the detection limit treatment affected ACSM statistics is in Fig. S4. During the entire study, the percentages of 30 min time points below the detection limit were 42% for organic aerosol and 2.1% for sulfate aerosol, and these increased to 46% and 4.7%, respectively, during just the marine periods discussed in what follows. ACSM data was not flagged for pollution as no statistically significant enhancement of organic and sulfate aerosol mass concentrations under polluted conditions was observed (Fig. S5). Sea surface temperature (SST) was recorded by a buoy approximately three nautical miles east of ENA (39° 05.208′ N, 27° 57.732′ W).[53] A near island chlorophyll-*a* time series was calculated from weekly MODIS chlorophyll-*a*,[54] and air mass back trajectories were computed with the Hybrid Single-Particle Lagrangian Integrated Trajectory (HYSPLIT) model.[55] Details on the supporting instrumentation and datasets are in Supporting Information S5.

3. RESULTS

3.1. Meteorology Overview and Assignment of Air Masses. Meteorological properties and ocean biogeochemical variables observed during the study period are presented in Fig. 1. The average and interquartile range of wind speed were

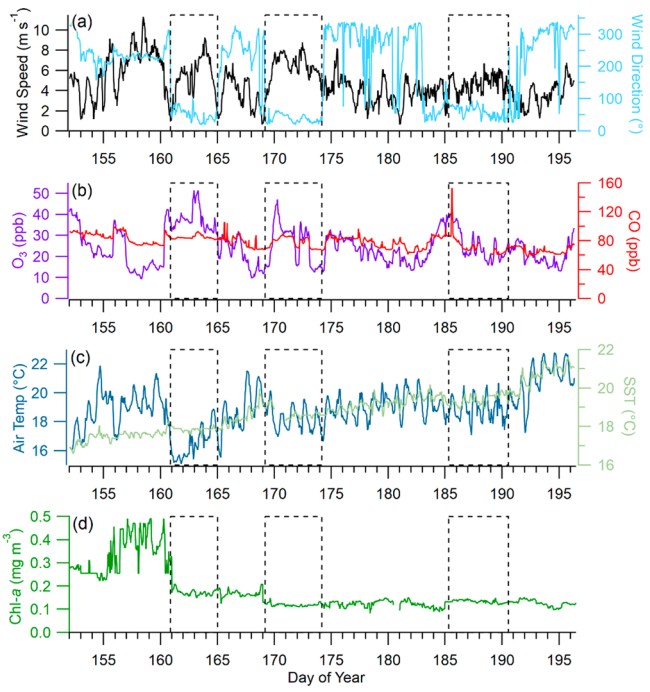

Figure 1. Study time series at 1 h averaging of (a) wind speed and wind direction, (b) O_3 and CO, (c) air temperature at ENA and SST near ENA, and (d) chlorophyll-*a* in the Azores region. Periods of marine air discussed throughout are boxed in dashed lines.

4.7 m s^{-1} (3.3−5.9 m s^{-1}), with maximums generally in the afternoons (13:00−16:00 UTC) (Fig. 1a). Winds most often originated from the north and southwest and rarely traversed the island from the southeast (Fig. 1a). O_3 did not exhibit a diurnal profile and measured 25 ppb (18−31 ppb) average and interquartile range; a few instances of much higher O_3, up to 51 ppb, were recorded, which could signify long-range transport or photochemical production (Fig. 1b). CO measured 78 ppb (70−84 ppb) average and interquartile range. Quick spikes in CO concentration were observed due to nearby anthropogenic activities but were mostly averaged out at 1 h time resolution (Fig. 1b). Both air temperature and SST

increased as the study progressed, ranging between 15−23 and 17−22 °C, respectively. Lastly, chlorophyll-*a*, derived from the near island MODIS time series, was low throughout the last 5 weeks, indicating minimal oceanic biological productivity detected by satellite in the surrounding ocean. The average and interquartile range of chlorophyll-*a* concentration was 0.18 mg m^{-3} (0.12−0.18 mg m^{-3}), which is characteristic for the Azores region during summer months.[56]

As discussed previously, MT has both terrestrial and oceanic sources and short atmospheric lifetimes, with the dominant oxidants at this site being OH and O_3. For an OH concentration of 2×10^6 molec. cm^{-3} and O_3 concentration of 25 ppb, when considering the four major observed isomers, MT lifetime can range 0.5−3 h at 298 K with respect to OH (bracketed by *β*-ocimene and *α*-pinene) and 1−20 h at 298 K with respect to O_3 (bracketed by *β*-ocimene and *β*-pinene). Due to minimal diurnal variability in boundary layer height at this site, the time-varying loss of VOC was primarily from oxidation. Periods of primarily marine and minimal terrestrial influence were determined by filtering for winds 330°−360° and 0°−90°, resulting in 44% of the data being classified as marine. This range in wind direction was set to keep the time of air traveling over land at the average wind speed to less than 10% of the lifetime of the most reactive observed isomer, *β*-ocimene. Given that air was sampled from a small island, making identification of marine periods by the inclusion of marine chemical tracers or exclusion of terrestrial chemical tracers difficult, we note that this is a best approximation for marine air masses, but there could still be some hyperlocal terrestrial influence affecting the data. Based on the wind filter, roughly 75% of the marine data fell in three distinct periods, with Period 1 corresponding to DOY 160.9−165, Period 2 corresponding to DOY 169.2−174.2, and Period 3 corresponding to DOY 185.3−190.5, highlighted in the boxed regions in Fig. 1 and in subsequent figures. Small wind shifts near the threshold resulted in 2% of Period 1 and 2.3% of Period 3 not passing the filter requirement but were included in the analysis. These three periods had distinct 48 h back trajectories, where Period 1 came from the west and later northeast, Period 2 came from directly north, and Period 3 came from the northeast. Representative back trajectories for each period are plotted over the June 2022 MODIS chlorophyll-*a* map in Fig. 2 and over the June 2022 MODIS SST map in Fig. S6. These trajectories were within the boundary layer for the previous 48 h. Since the MT lifetime is short, its biological production is most sensitively measured in the region close to ENA where there is little gradient in chlorophyll-*a* and SST.

3.2. BVOC Observations. The campaign time series of MT, isoprene, DMS, and MeSH is shown in Fig. 3. MT concentrations were highest in the early morning hours and lowest in the afternoons (Fig. 4a), indicating that its diurnal profile was primarily controlled by daytime OH oxidative removal rather than light- and temperature-dependent emission. Daily peak MT concentrations ranged considerably during the campaign, from 7.0 to 150 ppt, and averaged 20.0 ppt. We observed an increase in daily maximum MT concentrations in all air masses as the study progressed (Fig. 3a), which was coincident with increased SST and air temperatures. MT concentrations in marine air masses were typically lower than closely-matched time points in terrestrial air masses. The average MT concentration in the first two marine periods was 9 and 8 ppt and roughly three times higher at 25 ppt in the third period (Table 1). These total MT

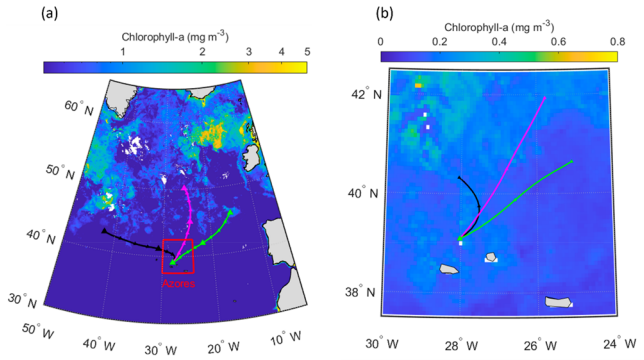

Figure 2. (a) Representative 48-hour back trajectories determined for the three periods of marine air overlaid on the June 2022 chlorophyll-a map collected by MODIS. The black trajectory arrived on DOY 161.5, the magenta trajectory arrived on DOY 171.5, and the green trajectory arrived on DOY 188.5. Large triangles represent 24-hour increments, and small triangles represent 6-hour increments. (b) Zoom in to 12-hour back trajectories corresponding to red inset box. Trajectory analysis was completed with the HYSPLIT model[55] using GDAS meteorological data as input.

concentrations are similar to Atlantic Ocean observations from the AMT22 cruise[35] and large swaths of the HiWinGS cruise.[34] They are also similar to the distant bloom measurements in Yassaa et al. (2008) where in-situ chlorophyll-*a* measured less than 0.5 mg m^{-3}, but they are at least an order of magnitude lower than the MT measurements made in more biologically active regions.

While the MT concentration was highly variable, we find that MT speciation was more stable across the entire campaign and between marine air masses. The colored background in Fig. 3a shows the fractions of the major identified MT isomers using GC-Vocus, which are reported for each period in Table 1. We observed a combination of endocyclic, exocyclic, and acyclic monoterpene isomers. During the first two marine periods where total MT concentration was low, MT speciation was comparable, with approximately 24% *α*-pinene, 40% *β*-pinene, and 32% combined limonene and *β*-ocimene. The *β*-pinene contribution increased to 52% during the third marine air period, and the remaining composition was roughly equally split between *α*-pinene and combined limonene and *β*-ocimene. Despite similar concentrations to those reported in Hackenberg et al. (2017), the major isomers in this study are different than their measurements, where the largest contributions were from limonene, ocimene, and myrcene. Our MT speciation most closely aligns with the distribution of speciated fluxes reported from the upwelling region off Peninsular Malaysia.[37] Despite atmospheric measurements of halogenated species like bromoform by the RT-Vocus (Fig. S7) and high concentrations of dissolved halides in the ocean, we did not find halogenated terpenes above the detection limit in this dataset.

Isoprene averaged 8.0 ppt across the entire study and showed a diurnal profile with near-zero concentrations in the early morning hours and maximums in the afternoons near 15:00 UTC (Fig. 4b), characteristic of its light- and temperature-dependent production pathways outweighing daytime oxidative loss. Because only three to four ambient chromatograms were collected daily, this diurnal profile in Fig. 3b appears as oscillating between the baseline and non-zero concentrations in some periods. Average isoprene concentrations during marine periods were 7.1, 6.9, and 12 ppt,

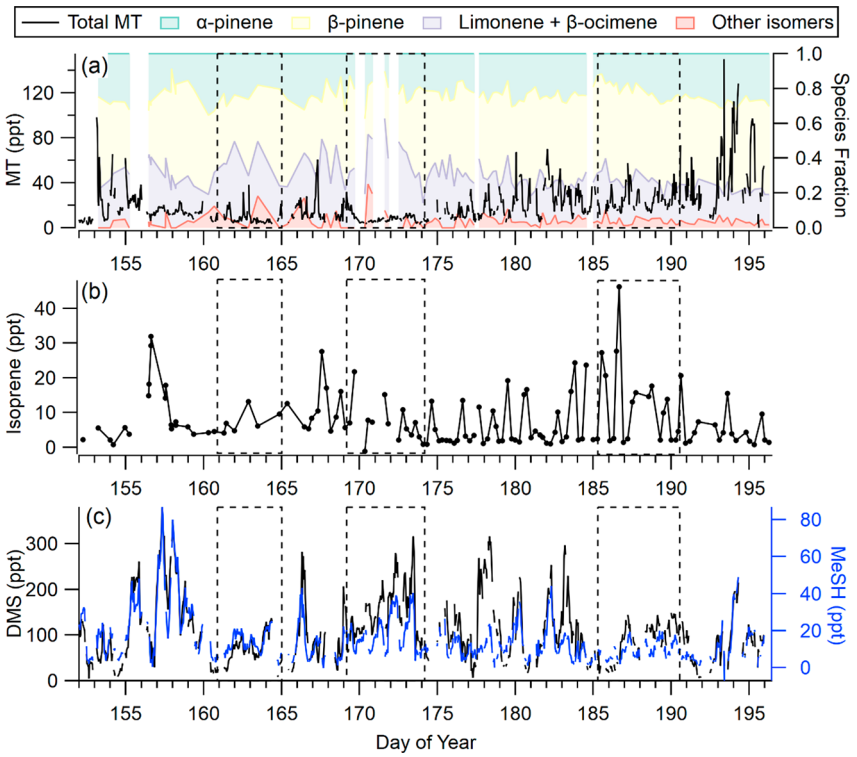

Figure 3. Study time series of (a) total MT measured by RT-Vocus and colored by fractional contribution of MT isomers measured by GC-Vocus, (b) isoprene measured by GC-Vocus, and (c) DMS and MeSH measured by the RT-Vocus. RT-Vocus measurements have pollution events filtered out.

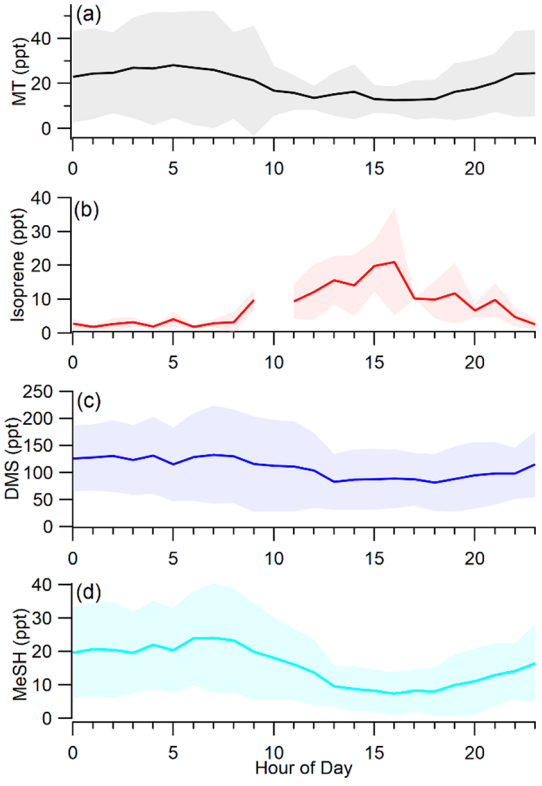

Figure 4. Campaign average diurnal profiles in local time for (a) MT, (b) isoprene, (c) DMS, and (d) MeSH. Diurnal profiles are averaged across all study days and not filtered for marine- or terrestrial-influenced periods. MT, DMS, and MeSH are from the RT-Vocus, and isoprene is from the GC-Vocus.

respectively, which is within the range of marine isoprene measurements reviewed by Shaw et al. (2010). Furthermore, these values closely align with more current remote marine isoprene measurements reported by Kim et al. (2017) in the Atlantic Ocean and Mungall et al. (2017) in the Arctic Ocean. Other field-based studies have observed correlations between isoprene and MT,[26,37] but given the contrasting diurnal profiles of isoprene and MT (Fig. 4), the significantly fewer data points available for isoprene quantifications, and lack of dissolved waterside measurements and sea to air fluxes, we were unable to draw conclusions on the potential correlation in this dataset. Contrary to previous laboratory studies measuring isoprene and MT production rates from phytoplankton monocultures[27,28] and field-based observations,[26,34,37] we measured consistently larger atmospheric MT concentrations than isoprene concentrations, with the average MT to isoprene ratio greater than 1 during all marine periods (Table 1). This could also be a result of the atmospheric lifetime. The Henry law and diffusion constants for isoprene and MT are similar ($0.029\ M\ atm^{-1}$ and $9.6 \times 10^6\ cm^2\ s^{-1}$ for isoprene and for one example, $0.050\ M\ atm^{-1}$ and $7.5 \times 10^6\ cm^2\ s^{-1}$ for β-pinene),[57,58] implying the dissolved concentration ratio in the ocean is directly related to the emission ratio. Isoprene reacts with OH faster than β-pinene, suggesting part of the discrepancy in MT to isoprene ratio compared to prior measurements could be attributed to atmospheric oxidative lifetime or an isoprene source farther than the MT source, resulting in lower isoprene concentrations measured at the site. Lastly, while we have carefully filtered the data for periods of primarily marine influence, given that the measurement site was located on an island and diurnal emission profiles of terrestrial and marine terpenes are expected to be similar, it is possible there was a hyperlocal terrestrial MT source that

Table 1. Trace Gas Concentrations and MT Speciation during Marine Periods 1, 2, and 3, and All Periods That Fit the Terrestrial Criteria[a]

Period	DOY	Total [MT] (ppt)	[MT] / [Isoprene]	[MT] / [DMS + MeSH]	Fraction α-pinene	Fraction β-pinene	Fraction Limonene + β-Ocimene	$[O_3]$ (ppb)
Marine 1	160.9−165.0	9 ± 6	1.7 (1.3−2.2)	0.16 (0.05−0.21)	0.25 ± 0.05	0.38 ± 0.10	0.30 ± 0.08	37 ± 5
Marine 2	169.2−174.2	8 ± 4	1.8 (0.7−2.9)	0.06 (0.04−0.06)	0.22 ± 0.07	0.41 ± 0.11	0.33 ± 0.11	26 ± 10
Marine 3	185.3−190.5	25 ± 9	6.2 (1.0−10.)	0.32 (0.18−0.37)	0.21 ± 0.05	0.52 ± 0.04	0.23 ± 0.04	25 ± 7
Terrestrial	DOY Fitting Terrestrial Criteria	23 ± 21	10. (1.8−9.9)	0.30 (0.09−0.35)	0.25 ± 0.05	0.46 ± 0.09	0.26 ± 0.07	22 ± 8

[a]Trace gas concentrations and speciation are reported as the average and standard deviation, whereas the two BVOC ratios are reported as the average and interquartile range. [MT]/[Isoprene] is based on linearly interpolating RT-Vocus MT to GC-Vocus isoprene time stamps.

inflated MT concentrations and contributed to the divergence relative to prior marine MT to isoprene ratios. It is difficult to determine the extent to which a terrestrial MT source might have influenced the dataset due to both marine and terrestrial terpenes having similar light- and temperature-dependent controls on their production.[27,59,60]

The campaign DMS and MeSH time series is shown in Fig. 3c. DMS and MeSH averaged 107 ± 69 and 15 ± 12 ppt, respectively, and were tightly correlated (R^2 = 0.60). The sum of DMS and MeSH did not track with MT during any marine periods, showing a weak negative correlation (R^2 = 0.13) during the first period, no correlation (R^2 = 0.01) during the second period, and a weak positive correlation (R^2 = 0.16) during the final period. These low correlation coefficients could be indicative of their different oceanic sources and biogeochemical controls and a result of the shorter MT lifetime relative to the dominant sulfur species, DMS. This was also apparent in the range in MT to (DMS+MeSH) ratios across all marine periods, which ranged 0.06−0.32 on average (Table 1). The variability in the MT to sulfur ratio has important implications for the formation, growth, and composition of secondary aerosol at this site and will be revisited in detail in Section 4.2.

4. DISCUSSION

4.1. Potential Controls on MT Speciation and Concentration. Here we evaluate how ocean biological and meteorological variables and atmospheric oxidation chemistry might have impacted the speciation and concentration of MT during marine periods at this site. The phytoplankton community in the Azores-region of the Eastern North Atlantic is dominated by coccolithophores, diatoms, and dinoflagellates in spring and summer months.[61−63] These phytoplankton species are known MT-producers with unique emission rates dependent on type and environmental stressors.[26,28] Additionally, the surrounding shore of Graciosa Island has documented occurrences of kelp species, which can be monoterpene producers and provide a near-shore source in line with our observations.[38,64] During summer months, the water is often oligotrophic,[56] in line with MODIS-derived chlorophyll-*a* during this study, and nutrient-limited dependent on mixed layer depth.[62] Without additional measurements of phytoplankton or macroalgal speciation and information about the stage of a potential bloom, we use the bulk MODIS-derived chlorophyll-*a* to hypothesize that there was a relatively low dissolved MT concentration and stable speciation during the first two marine periods. This could be a result of a low-producing phytoplankton or kelp community in the near-Azores region or efficient dissolved MT sinks. Since wind speeds were relatively low and constant preceding the third marine period, the increased MT concentration and different speciation during the third period is likely not reflective of changes in the mixed layer depth leading to vertical mixing and enhanced MT at the surface of the water column.

Instead, we suggest that the changing MT speciation and increased concentration during the third period is due to a directly offshore localized micro- or macroalgal bloom not detected by MODIS at 0.1° × 0.1° resolution and/or due to enhanced emissions from the warmer SST. Prior experiments showed α-pinene emission rates for the two diatom strains tested increased over the SST range observed here except during the low light conditions representative of nighttime conditions.[28] This experiment was only tested at two temperatures within our field observations, at 18 and 22 °C, so it is unclear whether this relationship can be explained mathematically. However, it is well-known that terrestrial MT emissions are analogously influenced by leaf temperature, and this temperature dependence can be described by an exponential relationship with coefficients specific to plant type.[65] We explore whether marine MT could have an exponential dependence on SST using the data points in the three marine periods, plotting the MT concentration as a function of SST in Fig. 5a and the MT concentration as a function of air temperature in Fig. 5b. MT concentration displayed an exponential relationship with SST with a moderate correlation (R^2 = 0.45), and total MT at higher SST had an increased contribution from the dominant isomer, β-pinene. Conversely, the MT concentration during the marine periods displayed a much weaker exponential correlation (R^2 = 0.09) with air temperature, lending credence to the expectation

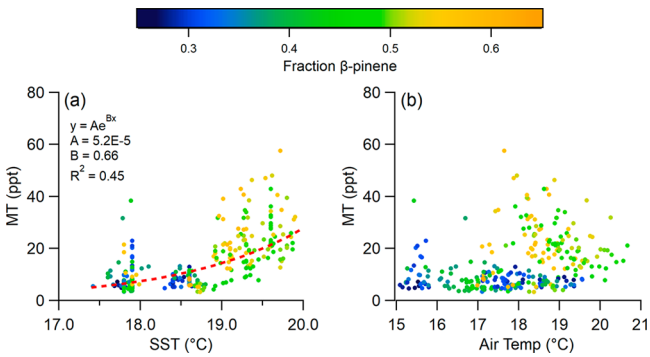

Figure 5. Regression of total MT concentration during the three discussed marine periods against (a) SST and (b) air temperature at ENA, both colored by the fraction of MT that is β-pinene. As the GC-Vocus did not simultaneously sample with RT-Vocus, the GC-Vocus β-pinene fraction was linearly interpolated to match RT-Vocus time points.

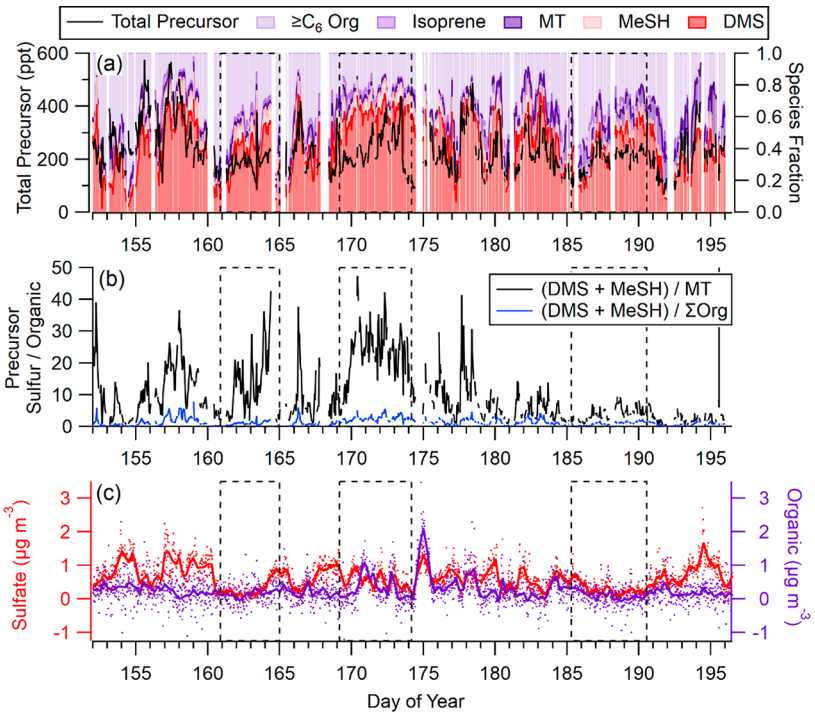

Figure 6. RT-Vocus study time series of (a) total aerosol precursor concentration in black and colored by fractional contribution of each precursor and (b) ratio of the sum of DMS and MeSH to MT in black and ratio of the sum of DMS and MeSH to sum of all organics in blue. GC isoprene was linearly interpolated to match RT time points. Trace gas ratios here represent a mole ratio. (c) ACSM study time series of sulfate and organic aerosol mass concentrations, where the dots represent 30 min data collection and lines represent 6-hour averages.

that MT in these air masses were primarily sourced from the ocean. Assuming constant dissolved concentrations and Henry's law constants dependent on temperature for the range 17−20 °C, and ignoring small enhancements in transfer velocity from greater diffusion over this narrow temperature range, we calculate a maximum 10−20% increase in airside concentration for all BVOC discussed. However, SST-dependences are not found for other BVOC reported in Fig. 3, leading us to believe that the relationship between MT concentration and SST could be a result of a biological process, such as phytoplankton stress.[28] The moderate SST-dependence reported here is in contrast to the findings of Hackenberg et al. (2017), where no relationship between MT and SST was observed across an approximately 30 °C SST range. Future field studies should further explore this relationship to determine whether it is robust across a wider SST range than observed in this study and across different oceanic regions and biogeochemical regimes.

Lastly, we explore whether ambient oxidation chemistry can explain the differences in MT concentration and speciation among the three marine periods in Table 1. Since this study occurred during consecutive 6 weeks and at a remote marine site, for the purpose of this discussion, we assume the average OH concentration is constant across study days[66] and the nitrate radical concentration is negligible. As a result, O_3 is the dominant variable influencing differences in ambient oxidation chemistry. If O_3 alone was responsible for varying MT concentration, then it would be expected that periods with high O_3 would have the lowest MT concentration and periods with similar O_3 would have approximately equivalent MT concentration. The difference in the level of O_3 was 11 ppb on average between periods 1 and 2, which is not large enough to observe detectable differences in MT concentrations beyond the variance in each period. However, the idea that ambient O_3 concentrations could be the sole driver of MT concentration differences is inconsistent with observations in periods 2 and 3, where the level of O_3 was approximately equivalent but the MT concentration was a factor of 3 different. Furthermore, if we prescribe a constant MT flux speciation and vary the amount of O_3 to match observations, the period experiencing the highest O_3 would have the greatest fraction of the least reactive isomer, β-pinene, which is again inconsistent with the measurements. While simple, these exercises demonstrate that some ocean biogeochemical control, rather than just atmospheric O_3 oxidation, is required to match measurements.

4.2. Contribution of MT to Secondary Aerosol. In the following section, the VOC measurements are discussed in the context of aerosol measurements at the site. We focus on VOC serving as aerosol precursors, which we define here as the sulfur species, DMS and MeSH, and organic species, including MT, isoprene, and other large organics (C_6 and greater),[67] and denoted as total aerosol precursor concentration. The collection of C_6 and larger organics were measured by the RT-Vocus at $C_xH_y^+$ and $C_xH_yO_z^+$ ions and were filtered based on an approximate detection limit, correlation to reduce overcounting fragments, and calibrated with the mean calibration factor to known quantified C_6 and larger organic molecules. Approximately half of the C_6 and larger organics were accounted for by five RT-Vocus ions consistent across marine periods (Fig. S8). The highest concentration ion contributors ($C_6H_{11}^+$, $C_7H_{13}^+$) corresponded to hexanal and heptanal, two aldehyde molecules which can have abiotic sources (Fig. S9).[18] The remaining organic precursor concentration was split among many ions equivalent to sub-ppt concentrations individually, resulting in their molecular information falling below the GC-Vocus detection limits.

The total aerosol precursor concentration throughout the study averaged 231 ± 86 ppt, with sulfur species 1.4 times greater than the collection of organic molecules on average (Fig. 6a,b). Monoterpenes notably comprised a minor fraction of the total detected organics (sum of isoprene, monoterpenes, and other C_6 and greater organics) (19 ± 13%) (Fig. 6a). This is also shown in Fig. 6b, where the ratio of sulfur species to MT was large and variable throughout the study, whereas the ratio of sulfur species to all aerosol precursor organics was considerably lower. The greater concentration of sulfate aerosol precursors compared to organic aerosol precursors aligned with aerosol measurements of sulfate and organic aerosol made by the ACSM at the site, shown in Fig. 6c. The ACSM aerosol measurements are interpreted as representative of secondary aerosol based on the following evidence: (1) the ACSM is largely insensitive to primary organic material in sea spray aerosol (SSA)[68] and non-SSA refractory aerosol as it cannot efficiently vaporize refractory aerosol,[51] and (2) primary SSA sampled by an aerosol mass spectrometer during low-oxidant seawater wave channel experiments had sulfate to organic ratios less than one,[69] which is in contrast to what was observed during this study where secondary aerosol is expected to be present. During this entire study, the average mass concentrations of sulfate and organic aerosol were 0.61 ± 0.40 and 0.32 ± 0.35 $\mu g\ m^{-3}$, respectively, and the mass ratio of sulfate to organic aerosol was consistently greater than one.

This dataset is further discussed for the marine periods boxed in Fig. 6. In the marine air masses studied, the mean and interquartile range of the mole ratio of sulfur to organic aerosol precursors was 1.6 (0.8−2.2) (Fig. 7a), and the mean and

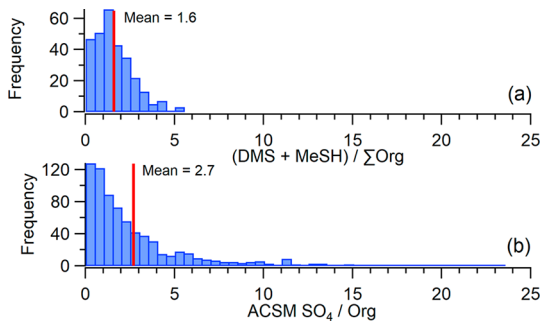

Figure 7. Histogram for all marine periods of (a) (DMS + MeSH) / sum of all organics measured by the RT-Vocus as a mole ratio and (b) sulfate to organic aerosol mass ratio measured by the ACSM where below detection limit points are filled with half the detection limit.

interquartile range of the mass ratio of measured sulfate to organic aerosol (Fig. 7b) was 2.7 (0.7−3.4). The measured sulfate to organic aerosol mass ratio in this study closely matched the value measured in the marine boundary layer during summer in the Northern Hemisphere as part of the ATom-1 campaign (2.4)[70] and in the Azores marine boundary layer during summer in the ACE-ENA study (3.1).[71]

A 0-D chemical box model built in the Framework for 0-Dimensional Atmospheric Modeling[72] was used to evaluate the extent to which MT, relative to other measured aerosol precursors, contributed to secondary aerosol in clean marine air masses. The model implemented chemistry from the Master Chemical Mechanism v3.3.1 and included reactions for MeSH oxidation and HPMTF formation and oxidation.[1] It was run with a static boundary layer height of 1000 m and a constant, first-order dilution term with a 2.3 day lifetime to approximate mixing out of the boundary layer. The model was initialized and constrained by the diurnal average of trace gas concentrations and meteorological measurements for the average of all of the marine air masses studied. Oxidation by nitrate and halogen radicals were assumed to be negligible at this site, so VOC were only oxidized by OH, with an assumed diurnal profile peaking at 3.3×10^6 molec. cm^{-3}, and O_3. Sulfate was formed by oxidation of MeSH, oxidation of DMS to SO_2 through the HPMTF intermediate, and via cloud uptake of HPMTF occurring at a rate of 1.2 h^{-1}.[73] It was assumed that no anthropogenic SO_2 was present, and long-range transport was negligible. SOA was formed by OH- and O_3-oxidation of MT and isoprene at a lower limit, using HOM yields,[21] and at an upper limit, using SOA yields (Table S3),[25,74] where formed SOA was estimated to have a molecular weight of 250 g mol^{-1}. The model was allowed to run continuously, and the sulfate/organic aerosol mass ratio was interpreted at steady-state. This analysis assumed that the representative marine air mass modeled was homogeneous over the aerosol lifetime.

We find that the mean modeled sulfate/organic aerosol mass ratio when the only aerosol precursors are DMS, MeSH, and speciated MT was 7.5 (interquartile range 7.0−7.9) at the lower limit and 1.6 (interquartile range 1.5−1.6) at the upper limit. A test including isoprene in addition to MT decreased the mean calculated sulfate/organic aerosol ratio by 1.5% to 7.4 and 16% to 1.3 at the lower and upper limits, respectively. These modeled outputs bracket the mean observations of the sulfate/organic aerosol mass ratio in the marine periods. We note that dominant pathways to SOA in the model at both limits are from the oxidation of limonene by OH (0.9−9.2% aerosol molar yield)[23,25] and O_3 (5.3−21.8% aerosol molar yield),[21,25] despite limonene constituting just 15% of the total MT concentration in the representative marine air mass. This highlights the importance of making speciated MT measurements to constrain SOA production in the marine atmosphere.

4.3. Outlook and Atmospheric Implications. MT measurements reported here add to an extremely limited suite of speciated MT measurements in the remote marine boundary layer and are the first in this region of the Atlantic Ocean. The short lifetime of MT results in measurements being exquisitely sensitive to near-island production, where ocean biogeochemical metrics exhibited little variability. Future work across wider biogeochemical and spatiotemporal regimes is needed to validate the exponential relationship observed between the SST and MT concentrations during this study. Additionally, the MT concentrations measured in this work are lower than those reported in Yassaa et al. (2008) and are more closely in line with those of Hackenberg et al. (2017). As such, our findings are more aligned with the global oceanic MT emission source proposed by Hackenberg et al. (2017) (0.16 Tg C yr^{-1}), which is at the low end of the current estimate range (0.01−29.5 Tg C yr^{-1}).[35,40] This should be further supported with future high-time-resolution flux measurements of marine MT to directly constrain MT emission inventories. Interestingly, the speciation measured here is much different than those for which global emission inventories are estimated, indicating that even if estimates for the carbon source term under typical oceanic conditions may be converging, the global impacts for atmospheric oxidation capacity and SOA still have considerable uncertainty. Lastly, our findings suggest that during this remote marine study, on average, marine organic aerosol is minor relative to sulfate aerosol, and SOA formed

from a small number of BVOC can potentially explain the observed sulfate/organic aerosol mass ratio.

■ ASSOCIATED CONTENT

Supporting Information

The Supporting Information is available free of charge at https://pubs.acs.org/doi/10.1021/acsestair.3c00112.

Details on VOC sampling and quantifications, pollution flag, and supporting measurements (PDF)

■ AUTHOR INFORMATION

Corresponding Author

Timothy H. Bertram − *Department of Chemistry, University of Wisconsin − Madison, Madison, Wisconsin 53706, United States;* orcid.org/0000-0002-3026-7588; Email: timothy.bertram@wisc.edu

Authors

Delaney B. Kilgour − *Department of Chemistry, University of Wisconsin − Madison, Madison, Wisconsin 53706, United States;* orcid.org/0000-0002-0435-9665

Christopher M. Jernigan − *Department of Chemistry, University of Wisconsin − Madison, Madison, Wisconsin 53706, United States;* Present Address: Cooperative Institute for Research in Environmental Sciences, University of Colorado Boulder, Boulder, CO 80305, USA; Present Address: NOAA Chemical Sciences Laboratory, Boulder, CO 80305, USA.; orcid.org/0000-0003-0302-5222

Shengqian Zhou − *Center for Aerosol Science and Engineering, Department of Energy, Environmental and Chemical Engineering, Washington University in St. Louis, St. Louis, Missouri 63130, United States*

Eduardo Brito de Azevedo − *Institute of Technology and Environmental Sciences (IITAA), University of the Azores, Angra do Heroísmo 9700-042, Portugal*

Jian Wang − *Center for Aerosol Science and Engineering, Department of Energy, Environmental and Chemical Engineering, Washington University in St. Louis, St. Louis, Missouri 63130, United States*

Maria A. Zawadowicz − *Environmental and Climate Sciences Department, Brookhaven National Laboratory, Upton, New York 11973, United States;* orcid.org/0000-0003-4234-0954

Complete contact information is available at: https://pubs.acs.org/10.1021/acsestair.3c00112

Notes

The authors declare the following competing financial interest(s): Tim Bertram is an associate editor.

■ ACKNOWLEDGMENTS

This material is based upon work supported by the U.S. Department of Energy (DOE), Office of Science, Office of Biological and Environmental Research, Atmospheric System Research (ASR) under Award No. DE-SC0021985. This research used resources of the Atmospheric Radiation Measurement (ARM) User Facility, which is a DOE Office of Science User Facility, under Award No. AFC010011. The authors thank the ARM staff at ENA and Los Alamos National Laboratory, including Bruno Cunha and Tercio Silva, for their support and logistical contributions to the study, and the ARM instrument mentors for providing publicly accessible supporting data from ENA. Additional thanks to Megan Claflin and Brian Lerner at Aerodyne Research, Inc. for discussions on quantitatively comparing RT-Vocus and GC-Vocus signals. NOAA Air Resources Laboratory is acknowledged for use of the HYSPLIT trajectory model.

■ REFERENCES

(1) Novak, G. A.; Kilgour, D. B.; Jernigan, C. M.; Vermeuel, M. P.; Bertram, T. H. Oceanic Emissions of Dimethyl Sulfide and Methanethiol and Their Contribution to Sulfur Dioxide Production in the Marine Atmosphere. *Atmos. Chem. Phys.* **2022**, *22* (9), 6309−6325.

(2) Carpenter, L. J.; Archer, S. D.; Beale, R. Ocean-Atmosphere Trace Gas Exchange. *Chem. Soc. Rev.* **2012**, *41* (19), 6473.

(3) Novak, G. A.; Bertram, T. H. Reactive VOC Production from Photochemical and Heterogeneous Reactions Occurring at the Air−Ocean Interface. *Acc. Chem. Res.* **2020**, *53* (5), 1014−1023.

(4) Donahue, N. M.; Prinn, R. G. Nonmethane Hydrocarbon Chemistry in the Remote Marine Boundary Layer. *J. Geophys. Res.* **1990**, *95* (D11), 18387.

(5) Meskhidze, N.; Xu, J.; Gantt, B.; Zhang, Y.; Nenes, A.; Ghan, S. J.; Liu, X.; Easter, R.; Zaveri, R. Global Distribution and Climate Forcing of Marine Organic Aerosol: 1. Model Improvements and Evaluation. *Atmos. Chem. Phys.* **2011**, *11* (22), 11689−11705.

(6) Fung, K. M.; Heald, C. L.; Kroll, J. H.; Wang, S.; Jo, D. S.; Gettelman, A.; Lu, Z.; Liu, X.; Zaveri, R. A.; Apel, E. C.; Blake, D. R.; Jimenez, J.-L.; Campuzano-Jost, P.; Veres, P. R.; Bates, T. S.; Shilling, J. E.; Zawadowicz, M. Exploring Dimethyl Sulfide (DMS) Oxidation and Implications for Global Aerosol Radiative Forcing. *Atmospheric Chemistry and Physics* **2022**, *22* (2), 1549−1573.

(7) Charlson, R. J.; Lovelock, J. E.; Andreae, M. O.; Warren, S. G. Oceanic Phytoplankton, Atmospheric Sulphur, Cloud Albedo and Climate. *Nature* **1987**, *326* (6114), 655−661.

(8) Gantt, B.; Xu, J.; Meskhidze, N.; Zhang, Y.; Nenes, A.; Ghan, S. J.; Liu, X.; Easter, R.; Zaveri, R. Global Distribution and Climate Forcing of Marine Organic Aerosol − Part 2: Effects on Cloud Properties and Radiative Forcing. *Atmospheric Chemistry and Physics* **2012**, *12* (14), 6555−6563.

(9) Prank, M.; Tonttila, J.; Ahola, J.; Kokkola, H.; Kühn, T.; Romakkaniemi, S.; Raatikainen, T. Impacts of Marine Organic Emissions on Low-Level Stratiform Clouds − a Large Eddy Simulator Study. *Atmospheric Chemistry and Physics* **2022**, *22* (16), 10971−10992.

(10) Hoffmann, E. H.; Tilgner, A.; Schrödner, R.; Bräuer, P.; Wolke, R.; Herrmann, H. An Advanced Modeling Study on the Impacts and Atmospheric Implications of Multiphase Dimethyl Sulfide Chemistry. *Proc. Natl. Acad. Sci. U. S. A.* **2016**, *113* (42), 11776−11781.

(11) Andreae, M. O.; Raemdonck, H. Dimethyl Sulfide in the Surface Ocean and the Marine Atmosphere: A Global View. *Science* **1983**, *221* (4612), 744−747.

(12) Andreae, M. O.; Ferek, R. J.; Bermond, F.; Byrd, K. P.; Engstrom, R. T.; Hardin, S.; Houmere, P. D.; LeMarrec, F.; Raemdonck, H.; Chatfield, R. B. Dimethyl Sulfide in the Marine Atmosphere. *Journal of Geophysical Research: Atmospheres* **1985**, *90* (D7), 12891−12900.

(13) Hulswar, S.; Simó, R.; Galí, M.; Bell, T. G.; Lana, A.; Inamdar, S.; Halloran, P. R.; Manville, G.; Mahajan, A. S. Third Revision of the Global Surface Seawater Dimethyl Sulfide Climatology (DMS-Rev3). *Earth System Science Data* **2022**, *14* (7), 2963−2987.

(14) Willis, M. D.; Burkart, J.; Thomas, J. L.; Köllner, F.; Schneider, J.; Bozem, H.; Hoor, P. M.; Aliabadi, A. A.; Schulz, H.; Herber, A. B.; Leaitch, W. R.; Abbatt, J. P. D. Growth of Nucleation Mode Particles in the Summertime Arctic: A Case Study. *Atmospheric Chemistry and Physics* **2016**, *16* (12), 7663−7679.

(15) Zheng, G.; Kuang, C.; Uin, J.; Watson, T.; Wang, J. Large Contribution of Organics to Condensational Growth and Formation of Cloud Condensation Nuclei (CCN) in the Remote Marine

Boundary Layer. *Atmospheric Chemistry and Physics* **2020**, *20* (21), 12515−12525.
(16) Zhou, S.; Gonzalez, L.; Leithead, A.; Finewax, Z.; Thalman, R.; Vlasenko, A.; Vagle, S.; Miller, L. A.; Li, S.-M.; Bureekul, S.; Furutani, H.; Uematsu, M.; Volkamer, R.; Abbatt, J. Formation of Gas-Phase Carbonyls from Heterogeneous Oxidation of Polyunsaturated Fatty Acids at the Air−Water Interface and of the Sea Surface Microlayer. *Atmos. Chem. Phys.* **2014**, *14* (3), 1371−1384.
(17) Ciuraru, R.; Fine, L.; van Pinxteren, M.; D'Anna, B.; Herrmann, H.; George, C. Photosensitized Production of Functionalized and Unsaturated Organic Compounds at the Air-Sea Interface. *Sci. Rep* **2015**, *5* (1), No. 12741.
(18) Schneider, S. R.; Collins, D. B.; Lim, C. Y.; Zhu, L.; Abbatt, J. P. D. Formation of Secondary Organic Aerosol from the Heterogeneous Oxidation by Ozone of a Phytoplankton Culture. *ACS Earth Space Chem.* **2019**, *3* (10), 2298−2306.
(19) Wang, Y.; Zeng, J.; Wu, B.; Song, W.; Hu, W.; Liu, J.; Yang, Y.; Yu, Z.; Wang, X.; Gligorovski, S. Production of Volatile Organic Compounds by Ozone Oxidation Chemistry at the South China Sea Surface Microlayer. *ACS Earth Space Chem.* **2023**, *7* (7), 1306−1313.
(20) Vermeuel, M. P.; Novak, G. A.; Kilgour, D. B.; Claflin, M. S.; Lerner, B. M.; Trowbridge, A. M.; Thom, J.; Cleary, P. A.; Desai, A. R.; Bertram, T. H. Observations of Biogenic Volatile Organic Compounds over a Mixed Temperate Forest during the Summer to Autumn Transition. *Atmospheric Chemistry and Physics* **2023**, *23* (7), 4123−4148.
(21) Jokinen, T.; Berndt, T.; Makkonen, R.; Kerminen, V.-M.; Junninen, H.; Paasonen, P.; Stratmann, F.; Herrmann, H.; Guenther, A. B.; Worsnop, D. R.; Kulmala, M.; Ehn, M.; Sipilä, M. Production of Extremely Low Volatile Organic Compounds from Biogenic Emissions: Measured Yields and Atmospheric Implications. *Proc. Natl. Acad. Sci. U. S. A.* **2015**, *112* (23), 7123−7128.
(22) Zhao, Y.; Thornton, J. A.; Pye, H. O. T. Quantitative Constraints on Autoxidation and Dimer Formation from Direct Probing of Monoterpene-Derived Peroxy Radical Chemistry. *Proc. Natl. Acad. Sci. U.S.A.* **2018**, *115* (48), 12142−12147.
(23) Ehn, M.; Thornton, J. A.; Kleist, E.; Sipilä, M.; Junninen, H.; Pullinen, I.; Springer, M.; Rubach, F.; Tillmann, R.; Lee, B.; Lopez-Hilfiker, F.; Andres, S.; Acir, I.-H.; Rissanen, M.; Jokinen, T.; Schobesberger, S.; Kangasluoma, J.; Kontkanen, J.; Nieminen, T.; Kurtén, T.; Nielsen, L. B.; Jørgensen, S.; Kjaergaard, H. G.; Canagaratna, M.; Maso, M. D.; Berndt, T.; Petäjä, T.; Wahner, A.; Kerminen, V.-M.; Kulmala, M.; Worsnop, D. R.; Wildt, J.; Mentel, T. F. A Large Source of Low-Volatility Secondary Organic Aerosol. *Nature* **2014**, *506* (7489), 476−479.
(24) Burkholder, J. B.; Sander, S. P.; Abbatt, J.; Barker, J. R.; Cappa, C.; Crounse, J. D.; Dibble, T. S.; Huie, R. E.; Kolb, C. E.; Kurylo, M. J.; Orkin, V. L.; Percival, C. J.; Wilmouth, D. M.; Wine, P. H. Chemical Kinetics and Photochemical Data for Use in Atmospheric Studies, Evaluation No. 19. *JPL Publication 19-5* 2019. http://jpldataeval.jpl.nasa.gov.
(25) Zhao, D. F.; Kaminski, M.; Schlag, P.; Fuchs, H.; Acir, I.-H.; Bohn, B.; Häseler, R.; Kiendler-Scharr, A.; Rohrer, F.; Tillmann, R.; Wang, M. J.; Wegener, R.; Wildt, J.; Wahner, A.; Mentel, T. F. Secondary Organic Aerosol Formation from Hydroxyl Radical Oxidation and Ozonolysis of Monoterpenes. *Atmospheric Chemistry and Physics* **2015**, *15* (2), 991−1012.
(26) Yassaa, N.; Peeken, I.; Zöllner, E.; Bluhm, K.; Arnold, S.; Spracklen, D.; Williams, J. Evidence for Marine Production of Monoterpenes. *Environ. Chem.* **2008**, *5* (6), 391.
(27) Shaw, S. L.; Gantt, B.; Meskhidze, N. Production and Emissions of Marine Isoprene and Monoterpenes: A Review. *Advances in Meteorology* **2010**, *2010*, 1−24.
(28) Meskhidze, N.; Sabolis, A.; Reed, R.; Kamykowski, D. Quantifying Environmental Stress-Induced Emissions of Algal Isoprene and Monoterpenes Using Laboratory Measurements. *Biogeosciences* **2015**, *12* (3), 637−651.
(29) Williams, J.; Yassaa, N.; Bartenbach, S.; Lelieveld, J. Mirror Image Hydrocarbons from Tropical and Boreal Forests. *Atmospheric Chemistry and Physics* **2007**, *7* (3), 973−980.
(30) Rinne, H. J. I.; Guenther, A. B.; Greenberg, J. P.; Harley, P. C. Isoprene and Monoterpene Fluxes Measured above Amazonian Rainforest and Their Dependence on Light and Temperature. *Atmospheric Environment* **2002**, *36* (14), 2421−2426.
(31) Hay, M. E.; Fenical, W. MARINE PLANT-HERBIVORE INTERACTIONS: The Ecology of Chemical Defense. *Annual Review of Ecology and Systematics* **1988**, *19* (1), 111−145.
(32) Wise, M. L. Monoterpene Biosynthesis in Marine Algae. *Phycologia* **2003**, *42* (4), 370−377.
(33) Lawson, S. J.; Selleck, P. W.; Galbally, I. E.; Keywood, M. D.; Harvey, M. J.; Lerot, C.; Helmig, D.; Ristovski, Z. Seasonal in Situ Observations of Glyoxal and Methylglyoxal over the Temperate Oceans of the Southern Hemisphere. *Atmospheric Chemistry and Physics* **2015**, *15* (1), 223−240.
(34) Kim, M. J.; Novak, G. A.; Zoerb, M. C.; Yang, M.; Blomquist, B. W.; Huebert, B. J.; Cappa, C. D.; Bertram, T. H. Air-Sea Exchange of Biogenic Volatile Organic Compounds and the Impact on Aerosol Particle Size Distributions: Air-Sea Exchange of Biogenic VOCs. *Geophys. Res. Lett.* **2017**, *44* (8), 3887−3896.
(35) Hackenberg, S. C.; Andrews, S. J.; Airs, R. L.; Arnold, S. R.; Bouman, H. A.; Cummings, D.; Lewis, A. C.; Minaeian, J. K.; Reifel, K. M.; Small, A.; Tarran, G. A.; Tilstone, G. H.; Carpenter, L. J. Basin-Scale Observations of Monoterpenes in the Arctic and Atlantic Oceans. *Environ. Sci. Technol.* **2017**, *51* (18), 10449−10458.
(36) Mungall, E. L.; Abbatt, J. P. D.; Wentzell, J. J. B.; Lee, A. K. Y.; Thomas, J. L.; Blais, M.; Gosselin, M.; Miller, L. A.; Papakyriakou, T.; Willis, M. D.; Liggio, J. Microlayer Source of Oxygenated Volatile Organic Compounds in the Summertime Marine Arctic Boundary Layer. *Proc. Natl. Acad. Sci. U. S. A.* **2017**, *114* (24), 6203−6208.
(37) Uning, R.; Latif, M. T.; Hamid, H. H. A.; Mohd Nadzir, M. S.; Khan, M. F.; Suratman, S. Sea-to-Air Fluxes of Isoprene and Monoterpenes in the Coastal Upwelling Region of Peninsular Malaysia. *ACS Earth Space Chem.* **2021**, *5*, 3429−3436.
(38) Tokarek, T. W.; Brownsey, D. K.; Jordan, N.; Garner, N. M.; Ye, C. Z.; Osthoff, H. D. Emissions of C9 − C16 Hydrocarbons from Kelp Species on Vancouver Island: Alaria Marginata (Winged Kelp) and Nereocystis Luetkeana (Bull Kelp) as an Atmospheric Source of Limonene. *Atmospheric Environment: X* **2019**, *2*, 100007.
(39) Tokarek, T. W.; Brownsey, D. K.; Jordan, N.; Garner, N. M.; Ye, C. Z.; Assad, F. V.; Peace, A.; Schiller, C. L.; Mason, R. H.; Vingarzan, R.; Osthoff, H. D. Biogenic Emissions and Nocturnal Ozone Depletion Events at the Amphitrite Point Observatory on Vancouver Island. *Atmosphere-Ocean* **2017**, *55* (2), 121−132.
(40) Luo, G.; Yu, F. A Numerical Evaluation of Global Oceanic Emissions of α-Pinene and Isoprene. *Atmos. Chem. Phys.* **2010**, *10*, 2007−2015.
(41) Krechmer, J.; Lopez-Hilfiker, F.; Koss, A.; Hutterli, M.; Stoermer, C.; Deming, B.; Kimmel, J.; Warneke, C.; Holzinger, R.; Jayne, J.; Worsnop, D.; Fuhrer, K.; Gonin, M.; de Gouw, J. Evaluation of a New Reagent-Ion Source and Focusing Ion−Molecule Reactor for Use in Proton-Transfer-Reaction Mass Spectrometry. *Anal. Chem.* **2018**, *90* (20), 12011−12018.
(42) Claflin, M. S.; Pagonis, D.; Finewax, Z.; Handschy, A. V.; Day, D. A.; Brown, W. L.; Jayne, J. T.; Worsnop, D. R.; Jimenez, J. L.; Ziemann, P. J.; de Gouw, J.; Lerner, B. M. An in Situ Gas Chromatograph with Automatic Detector Switching between PTR- and EI-TOF-MS: Isomer-Resolved Measurements of Indoor Air. *Atmospheric Measurement Techniques* **2021**, *14* (1), 133−152.
(43) Bertram, T. H.; Kimmel, J. R.; Crisp, T. A.; Ryder, O. S.; Yatavelli, R. L. N.; Thornton, J. A.; Cubison, M. J.; Gonin, M.; Worsnop, D. R. A Field-Deployable, Chemical Ionization Time-of-Flight Mass Spectrometer. *Atmospheric Measurement Techniques* **2011**, *4* (7), 1471−1479.
(44) Claflin, M. S.; Lerner, B. M. Quantitative Comparison of Direct and GC-Speciated CI-TOF-MS Measurements. In *Zenodo*. DOI: 10.5281/zenodo.10069422 (accessed 2023-11-03).

(45) Uin, J.; Aiken, A. C.; Dubey, M. K.; Kuang, C.; Pekour, M.; Salwen, C.; Sedlacek, A. J.; Senum, G.; Smith, S.; Wang, J.; Watson, T. B.; Springston, S. R. Atmospheric Radiation Measurement (ARM) Aerosol Observing Systems (AOS) for Surface-Based In Situ Atmospheric Aerosol and Trace Gas Measurements. *Journal of Atmospheric and Oceanic Technology* **2019**, *36* (12), 2429−2447.
(46) Zawadowicz, M.; Howie, J.; Shilling, J.; Levin, M. ARM Data Center. *ACSM, Corrected for Composition-Dependent Collection Efficiency (ACSMCDCE)*; Eastern North Atlantic (ENA) DOI: 10.5439/1763029 (accessed 2023-08-01).
(47) Koontz, A.; Springston, S.; Trojanowski, R. ARM Data Center. *Carbon Monoxide Analyzer (AOSCO).*; Eastern North Atlantic (ENA) DOI: 10.5439/1250819 (accessed 2023-08-01).
(48) Springston, S.; Koontz, A.; Trojanowski, R. ARM Data Center. *Ozone Monitor (AOSO3).*; Eastern North Atlantic (ENA). DOI: 10.5439/1346692 (accessed 2023-08-01).
(49) Kyrouac, J.; Springston, S.; Tuftedal, M. ARM Data Center. *Meteorological Measurements Associated with the Aerosol Observing System (AOSMET).*; Eastern North Atlantic (ENA) DOI: 10.5439/1984920 (accessed 2023-08-01).
(50) Shilling, J. E.; Levin, M. S. *Aerosol Chemical Speciation Monitor (ACSM) Composition-Dependent Collection Efficiency (CDCE) Value-Added Product Report*; U.S. Department of Energy Office of Scientific and Technical Information, 2021.
(51) Ng, N. L.; Herndon, S. C.; Trimborn, A.; Canagaratna, M. R.; Croteau, P. L.; Onasch, T. B.; Sueper, D.; Worsnop, D. R.; Zhang, Q.; Sun, Y. L.; Jayne, J. T. An Aerosol Chemical Speciation Monitor (ACSM) for Routine Monitoring of the Composition and Mass Concentrations of Ambient Aerosol. *Aerosol Science and Technology* **2011**, *45* (7), 780−794.
(52) Kim, E.; Hopke, P. K.; Edgerton, E. S. Source Identification of Atlanta Aerosol by Positive Matrix Factorization. *J. Air Waste Manage. Assoc.* **2003**, *53* (6), 731−739.
(53) Azevedo, E. B.; Reis, F. V.; Tomé, R. D.; Simões, A. T.; Valente, A. S.; Rodrigues, M. C. CLIMAAT Project. Integrated Meteo-Oceanographic Support System for Ports in the Azores. In *Proceedings of the 2nd Hydrographic Engineering Conference;* CMMG: Lisbon, Portugal, 2012.
(54) NASA Goddard Space Flight Center. MODIS-Aqua Ocean Color Data, 2022. https://neo.gsfc.nasa.gov/view.php?datasetId=MY1DMM_CHLORA&year=2022 (accessed 2023-11-14).
(55) Stein, A. F.; Draxler, R. R.; Rolph, G. D.; Stunder, B. J. B.; Cohen, M. D.; Ngan, F. NOAA's HYSPLIT Atmospheric Transport and Dispersion Modeling System. *Bulletin of the American Meteorological Society* **2015**, *96* (12), 2059−2077.
(56) Caldeira, R. M. A.; Reis, J. C. The Azores Confluence Zone. *Frontiers in Marine Science* **2017**, *4* (37). DOI: 10.3389/fmars.2017.00037.
(57) Karl, T.; Yeretzian, C.; Jordan, A.; Lindinger, W. Dynamic Measurements of Partition Coefficients Using Proton-Transfer-Reaction Mass Spectrometry (PTR−MS). *International Journal of Mass Spectrometry* **2003**, *223−224*, 383−395.
(58) Gharagheizi, F. Determination of Diffusion Coefficient of Organic Compounds in Water Using a Simple Molecular-Based Method. *Ind. Eng. Chem. Res.* **2012**, *51* (6), 2797−2803.
(59) Malik, A. H.; Iyer, P. K. Conjugated Polyelectrolyte Based Sensitive Detection and Removal of Antibiotics Tetracycline from Water. *ACS Appl. Mater. Interfaces* **2017**, *9* (5), 4433−4439.
(60) Broadgate, W. J.; Malin, G.; Küpper, F. C.; Thompson, A.; Liss, P. S. Isoprene and Other Non-Methane Hydrocarbons from Seaweeds: A Source of Reactive Hydrocarbons to the Atmosphere. *Marine Chemistry* **2004**, *88* (1), 61−73.
(61) Silva, A.; Brotas, V.; Valente, A.; Sá, C.; Diniz, T.; Patarra, R. F.; Álvaro, N. V.; Neto, A. I. Coccolithophore Species as Indicators of Surface Oceanographic Conditions in the Vicinity of Azores Islands. *Estuarine, Coastal and Shelf Science* **2013**, *118*, 50−59.
(62) Barcelos E Ramos, J.; Schulz, K. G.; Voss, M.; Narciso, Á.; Müller, M. N.; Reis, F. V.; Cachão, M.; Azevedo, E. B. Nutrient-Specific Responses of a Phytoplankton Community: A Case Study of the North Atlantic Gyre, Azores. *Journal of Plankton Research* **2017**, *39* (4), 744−761.
(63) Santos, M.; Moita, M. T.; Bashmachnikov, I.; Menezes, G. M.; Carmo, V.; Loureiro, C. M.; Mendonça, A.; Silva, A. F.; Martins, A. Phytoplankton Variability and Oceanographic Conditions at Condor Seamount, Azores (NE Atlantic). *Deep Sea Research Part II: Topical Studies in Oceanography* **2013**, *98*, 52−62.
(64) Tempera, F.; Milla-Figueras, D.; Sinde-Mano, A. L.; Atchoi, E.; Afonso, P. Range Extension of Mesophotic Kelps (Ochrophyta: Laminariales and Tilopteridales) in the Central North Atlantic: Opportunities for Marine Forest Research and Conservation. *Journal of Phycology* **2021**, *57* (4), 1140−1150.
(65) Guenther, A. B.; Zimmerman, P. R.; Harley, P. C.; Monson, R. K.; Fall, R. Isoprene and Monoterpene Emission Rate Variability: Model Evaluations and Sensitivity Analyses. *Journal of Geophysical Research: Atmospheres* **1993**, *98* (D7), 12609−12617.
(66) Spivakovsky, C. M.; Logan, J. A.; Montzka, S. A.; Balkanski, Y. J.; Foreman-Fowler, M.; Jones, D. B. A.; Horowitz, L. W.; Fusco, A. C.; Brenninkmeijer, C. a. M.; Prather, M. J.; Wofsy, S. C.; McElroy, M. B. Three-Dimensional Climatological Distribution of Tropospheric OH: Update and Evaluation. *Journal of Geophysical Research: Atmospheres* **2000**, *105* (D7), 8931−8980.
(67) Donahue, N. M.; Epstein, S. A.; Pandis, S. N.; Robinson, A. L. A Two-Dimensional Volatility Basis Set: 1. Organic-Aerosol Mixing Thermodynamics. *Atmospheric Chemistry and Physics* **2011**, *11* (7), 3303−3318.
(68) Freney, E.; Sellegri, K.; Nicosia, A.; Williams, L. R.; Rinaldi, M.; Trueblood, J. T.; Prévôt, A. S. H.; Thyssen, M.; Grégori, G.; Haëntjens, N.; Dinasquet, J.; Obernosterer, I.; Van Wambeke, F.; Engel, A.; Zäncker, B.; Desboeufs, K.; Asmi, E.; Timonen, H.; Guieu, C. Mediterranean Nascent Sea Spray Organic Aerosol and Relationships with Seawater Biogeochemistry. *Atmospheric Chemistry and Physics* **2021**, *21* (13), 10625−10641.
(69) Sauer, J. S.; Mayer, K. J.; Lee, C.; Alves, M. R.; Amiri, S.; Bahaveolos, C. J.; Franklin, E. B.; Crocker, D. R.; Dang, D.; Dinasquet, J.; Garofalo, L. A.; Kaluarachchi, C. P.; Kilgour, D. B.; Mael, L. E.; Mitts, B. A.; Moon, D. R.; Moore, A. N.; Morris, C. K.; Mullenmeister, C. A.; Ni, C.-M.; Pendergraft, M. A.; Petras, D.; Simpson, R. M. C.; Smith, S.; Tumminello, P. R.; Walker, J. L.; DeMott, P. J.; Farmer, D. K.; Goldstein, A. H.; Grassian, V. H.; Jaffe, J. S.; Malfatti, F.; Martz, T. R.; Slade, J. H.; Tivanski, A. V.; Bertram, T. H.; Cappa, C. D.; Prather, K. A. The Sea Spray Chemistry and Particle Evolution Study (SeaSCAPE): Overview and Experimental Methods. *Environ. Sci.: Processes Impacts* **2022**, *24* (2), 290−315.
(70) Hodzic, A.; Campuzano-Jost, P.; Bian, H.; Chin, M.; Colarco, P. R.; Day, D. A.; Froyd, K. D.; Heinold, B.; Jo, D. S.; Katich, J. M.; Kodros, J. K.; Nault, B. A.; Pierce, J. R.; Ray, E.; Schacht, J.; Schill, G. P.; Schroder, J. C.; Schwarz, J. P.; Sueper, D. T.; Tegen, I.; Tilmes, S.; Tsigaridis, K.; Yu, P.; Jimenez, J. L. Characterization of Organic Aerosol across the Global Remote Troposphere: A Comparison of ATom Measurements and Global Chemistry Models. *Atmospheric Chemistry and Physics* **2020**, *20* (8), 4607−4635.
(71) Zawadowicz, M. A.; Suski, K.; Liu, J.; Pekour, M.; Fast, J.; Mei, F.; Sedlacek, A. J.; Springston, S.; Wang, Y.; Zaveri, R. A.; Wood, R.; Wang, J.; Shilling, J. E. Aircraft Measurements of Aerosol and Trace Gas Chemistry in the Eastern North Atlantic. *Atmos. Chem. Phys.* **2021**, *21* (10), 7983−8002.
(72) Wolfe, G. M.; Marvin, M. R.; Roberts, S. J.; Travis, K. R.; Liao, J. The Framework for 0-D Atmospheric Modeling (F0AM) v3.1. *Geoscientific Model Development* **2016**, *9* (9), 3309−3319.
(73) Novak, G. A.; Fite, C. H.; Holmes, C. D.; Veres, P. R.; Neuman, J. A.; Faloona, I.; Thornton, J. A.; Wolfe, G. M.; Vermeuel, M. P.; Jernigan, C. M.; Peischl, J.; Ryerson, T. B.; Thompson, C. R.; Bourgeois, I.; Warneke, C.; Gkatzelis, G. I.; Coggon, M. M.; Sekimoto, K.; Bui, T. P.; Dean-Day, J.; Diskin, G. S.; DiGangi, J. P.; Nowak, J. B.; Moore, R. H.; Wiggins, E. B.; Winstead, E. L.; Robinson, C.; Thornhill, K. L.; Sanchez, K. J.; Hall, S. R.; Ullmann, K.; Dollner, M.; Weinzierl, B.; Blake, D. R.; Bertram, T. H. Rapid Cloud Removal of Dimethyl Sulfide Oxidation Products Limits SO2

and Cloud Condensation Nuclei Production in the Marine Atmosphere. *Proc. Natl. Acad. Sci. U.S.A.* **2021**, *118* (42), No. e2110472118.
(74) Clark, C. H.; Kacarab, M.; Nakao, S.; Asa-Awuku, A.; Sato, K.; Cocker, D. R. I. Temperature Effects on Secondary Organic Aerosol (SOA) from the Dark Ozonolysis and Photo-Oxidation of Isoprene. *Environ. Sci. Technol.* **2016**, *50* (11), 5564−5571.